Solid State Ionics 373 (2021) 115814

Contents lists available at ScienceDirect

Solid State Ionics

journal homepage: www.elsevier.com/locate/ssi

Mechanistic insights into the dry prelithiated WO_3 thin films in electrochromic devices

Zhenhua Wang [a,b], Liaolin Zhang [a], Hongliang Zhang [b,c,*], Ran Jiang [d], Lingyan Liang [b], Junhua Gao [b], Hongtao Cao [b,c,*]

[a] School of Material Science and Engineering, Jiangxi University of Science and Technology, Ganzhou 341000, China
[b] Laboratory of Advanced Nano Materials and Devices, Ningbo Institute of Materials Technology and Engineering, Chinese Academy of Sciences, Ningbo 315201, China
[c] Center of Materials Science and Optoelectronics Engineering, University of Chinese Academy of Sciences, Beijing 100049, China
[d] School of Information Science and Engineering, Ningbo University, Ningbo 315211, China

ARTICLE INFO

Keywords:
Dry prelithiation
Tungsten oxide
Electrochromic devices
Cycling stability

ABSTRACT

While the dry prelithiation method has been extensively applied in WO_3-based electrochromic devices, the insight of prelithiated WO_3 films is still ambiguous. Herein, the electrochromic and electrochemical performance of the WO_3 films prepared by an in situ dry prelithiation method is investigated. The deposited lithium is calculated to be separated into 47.8% 'active lithium' and 52.2% 'dead lithium'. On one hand, the enhancement of the electrochemical cycling stability and charge density can be ascribed to the preactivation of 'active lithium', which enlarges the surface area for ion transporting. On the other, the irreversible formation of 'dead lithium zone' in the prelithiated WO_3 films originates from 'dead lithium seed', leading to the detriment of optical properties. This work further provides a profound insight into the implication of prelithiated lithium on the electrochemical and electrochromic properties of the WO_3 films.

1. Introduction

Prelithiation as an effective strategy of compensating for extra lithium has been receiving widespread attention in the application of electrochromic devices (ECDs) [1–3], lithium-ion battery [4–6] and lithium-ion capacitor [7,8]. In terms of electrochromic devices, the prelithiation can be subdivided into wet lithiation and dry lithiation based on the different preparation strategies. The intercalation of lithium induced by wet lithiation is realized by the electrochemical cycling of the material in Li^+-based solution [9,10]. Dry lithiation is carried out by exposing the material to lithium atoms vapor in a dry vacuum environment [11–13]. Tungsten oxide (WO_3) has been demonstrated to be a promising inorganic material as the electrochromic cathode due to its large optical transmittance and high coloration efficiency [14,15]. Recently, the dry lithiation technique, known as its advantage of facile preparation and no cleaning the samples, has been widely used to investigate the electrochromic characteristic of the WO_3 films in all-solid-state electrochromic devices. As reported in previous literature, dry lithiation has been introduced to intercalate various thickness of lithium into the nanostructured WO_3 films, demonstrating that the amount of predeposited lithium plays a vital role in coloration efficiency [16]. Very recently, a novel type of all-solid-state electrochromic device glass/ITO/NiO/ZrO_2/prelithiated-WO_3/ITO by multi-target electron beam evaporation has reported to enjoy a large transmittance modulation of 52.5% and a high coloration efficiency of 106.6 $cm^2\ C^{-1}$ at 550 nm [17]. Another all-solid-state ECD glass/ITO/WO_3/Ta_2O_5/Ni-V-O/ITO fabricated using in-vacuo dry lithiation method at magnetron sputtering system has demonstrated excellent properties with a coloration efficiency of 63.0 $cm^2\ C^{-1}$ and a transmittance modulation of about 40% [18]. Despite the progress, the effect of prelithiation on the electrochromic and electrochemical properties of the WO_3 films still remains to be further explained, which restricts the advancement of ECDs.

Herein, mechanistic insights into the dry prelithiated WO_3 thin films deposited by the one step electron beam evaporation in electrochromic devices is investigated. This investigation aims to obtain a scientific understanding of the electrochromic behavior caused by preintroducing extra lithium.

* Corresponding authors at: Laboratory of Advanced Nano Materials and Devices, Ningbo Institute of Materials Technology and Engineering, Chinese Academy of Sciences, Ningbo 315201, China.
E-mail addresses: zhanghl@nimte.ac.cn (H. Zhang), h_cao@nimte.ac.cn (H. Cao).

https://doi.org/10.1016/j.ssi.2021.115814
Received 26 September 2021; Received in revised form 1 November 2021; Accepted 14 November 2021
Available online 19 November 2021

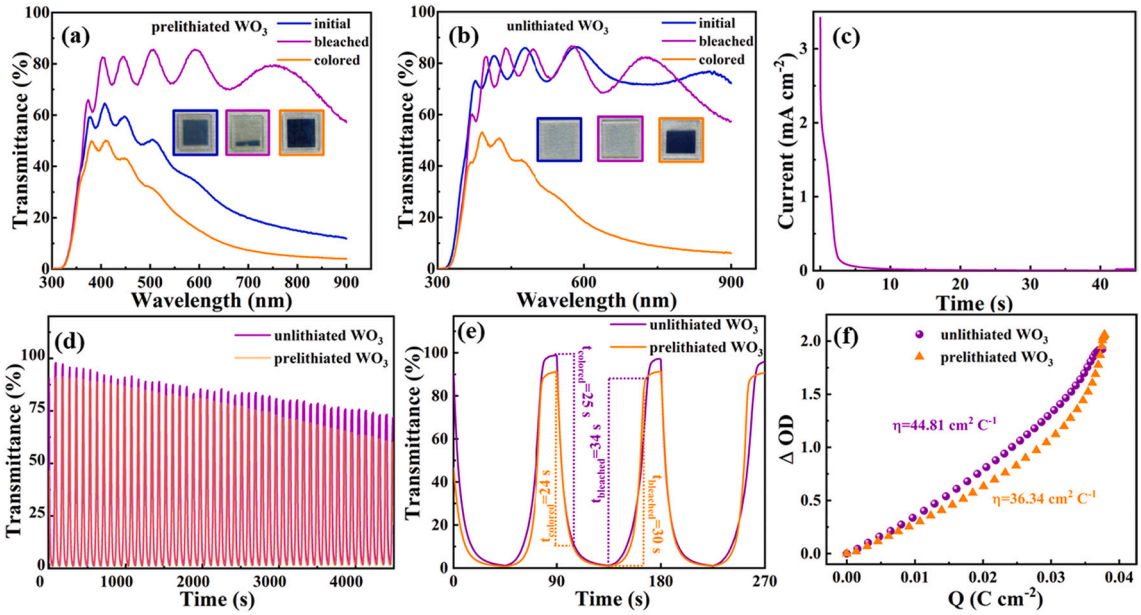

Fig. 1. The optical transmittance spectra of the (a) prelithiated and (b) unlithiated WO_3 films in the wavelength range from 300 to 900 nm. (c) The current density curve of the prelithiated WO_3 films during the deintercalation of Li. (d)-(e) The in situ transmittance spectra monitored at λ_{633nm} (−1.0 V/+1.0 V, per cycle) for the prelithiated and unlithiated WO_3 films in 0.1 M Li^+-based electrolyte. (f) The curves of in situ optical density change as a function of charge density per unit area at λ_{633nm} for the prelithiated and unlithiated WO_3 films.

2. Preparation of the individual films and assembly of electrochromic device

These individual films were prepared in a vacuum background pressure of less than 2.0×10^{-3} Pa via an electron beam evaporation method (MUE-ECO made ULVAC, Japan). The WO_3 films with a thickness of 350 nm were deposited on indium tin oxide (ITO) covered glass at a substrate temperature of 200 °C. The growth rate and deposition power were 1–2 Å and about 5 W, respectively. Subsequently, the extra lithium was in situ grown on the deposited WO_3 films by exposing the WO_3 films in vacuum containing lithium vapor atoms. The thickness and deposition rate of the prelithiated lithium was 10 nm (observed by a quartz crystal thickness monitor) and 0.3–0.6 Å, respectively. Analogously, the NiO thin films as an ion-storage layer were deposited onto the ITO-coated glass at room temperature using the same technique. Then, the as-deposited NiO thin films were annealed at 300 °C for 1 h in air. The electrochromic devices with the configuration of ITO/ the unlithiated WO_3/Li^+-based electrolyte/NiO/ITO and ITO/the prelithiated WO_3/Li^+-based electrolyte/NiO/ITO were assembled by pouring 0.1 M PC-$LiClO_4$ electrolytes between these two individual films during the process of vacuum packaging.

3. Characterization

The electrochromic performances of the WO_3 films and the prelithiated WO_3 films were measured by an electrochemical workstation (CHI660D, Chenhua, Shanghai). The electrochemical measurements were conducted in 0.1 M $LiClO_4$-propylene carbonate (PC) electrolyte solution using a three-electrode system composed of the films (working electrode), a platinum sheet (counter electrode) and $Hg/HgCl_2$ (reference electrode). UV-vis-IR spectroscopy combined with an electrochemical workstation was applied to obtain the ex situ and in situ transmittance spectra of the WO_3 films and prelithiated WO_3 films. The electrochemical impedance spectra were characterized by an electrochemical workstation (Zennium, IM6) in the frequency range from 100 mHz to 100 kHz.

4. Results and discussion

Lithium with a thickness of about 10 nm was deposited on the WO_3 films by in situ dry lithiation method to investigate the effect of predeposited lithium on the optical performance of the WO_3 films. After deduction of an air background, the measured ex situ optical transmittance spectra of the prelithiated and unlithiated WO_3 films is shown in Fig. 1 (a) and (b), respectively. The prelithiated WO_3 films (as shown in the insets of Fig. 1 (a)) show a visual appearance of light blue accompanying transmittance variation from 77.8% to 27.6% at 633 nm, implying that the insertion of lithium can result in the detriment of transmittance. It is noted that a distinct optical transmittance difference between initial state and bleached state is observed, which can be attributed to incomplete restoration of the initial interface of the WO_3 films and Li^+-based electrolyte, originating partly from an irreversible insertion of lithium-ion. The deposited lithium can be separated into 'dead lithium' (irreversibly bound in the framework of WO_3 films) and 'active lithium' (freely extracted from the substrate). To quantitatively analyze the composition of deposited lithium, chronoamperometry measurement was carried out in 0.1 M $LiClO_4$-PC electrolyte to extract 'active lithium'. Fig. 1 (c) shows that the current density of prelithiated WO_3 films is dropped from 3.42 mA cm^{-2} to almost zero, indicating the extraction of 'active lithium' [17]. The theoretical value of 'active lithium' is determined to be 3.55 mC cm^{-2} by integrating the CA curve. Based on the equivalence relationship between extracted charge and deintercalated 'active lithium', the extracted thickness of 'active lithium' can be calculated by [17]:

$$h = \frac{V}{S} = \frac{m}{\rho \times S} = \frac{n \times M}{\rho \times S} \quad (1)$$

$$n = \frac{Q \times 6.24146 \times 10^{18}}{N_A} \quad (2)$$

where h, S, V, m, ρ and n presents thickness, area, volume, mass, density and amount of substance, respectively. Q, N_A and 6.24146×10^{18} refers to the amount of charge, Avogadro constant and the number of electrons per coulomb, respectively. The thickness of 'active lithium' is calculated to be 4.78 nm, implying that 47.8% of 'active lithium' and 52.2% of

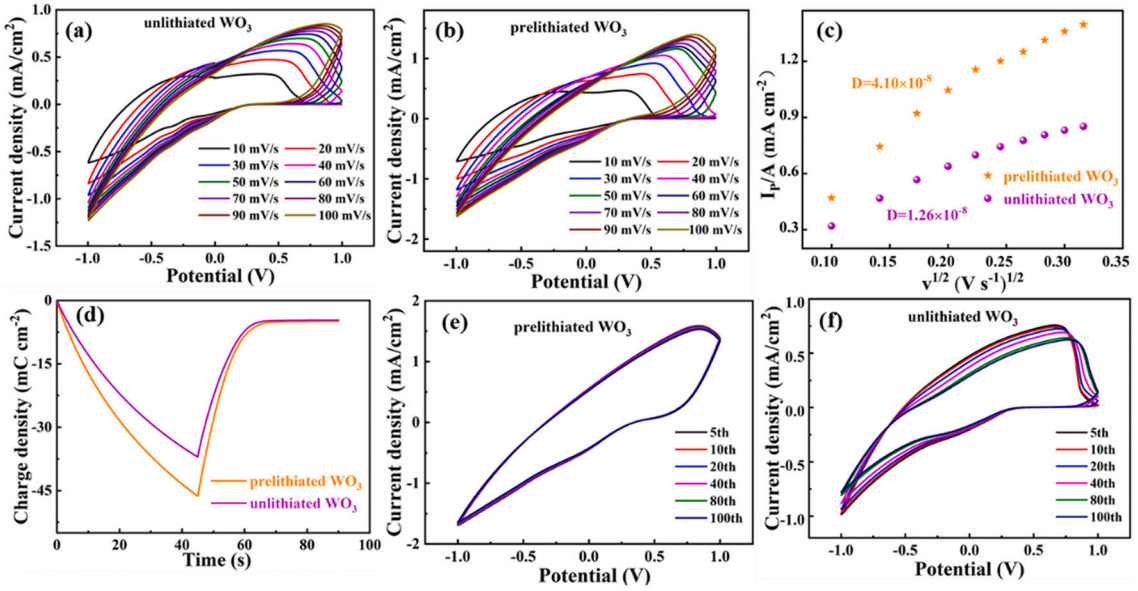

Fig. 2. Cyclic voltammograms (CV) plots of the (a) prelithiated and (b) unlithiated WO_3 films. (c) The plots of the peak current densities (I_p) as a function of the square root of scan rate ($v^{1/2}$) in the prelithiated and unlithiated WO_3 films. (d) The charge density for the prelithiated and unlithiated WO_3 films in 0.1 M PC-$LiClO_4$ electrolyte. Initial 100 CV curves of the (e) prelithiated and (f) unlithiated WO_3 films at the scan rate of 100 mV/s.

'dead lithium' are codistributed in the framework of the prelithiated WO_3 films. Fig. 1 (d) displays the sets of in situ time-dependent transmittance spectra (measured by subtracting the total background of the reaction tank and the $LiClO_4$-PC solution) of the prelithiated and unlithiated WO_3 films at 633 nm, alternately measured at +1.0 V/−1.0 V for 45 s. The maximum transmittance modulation (ΔT, colored-state/bleached-state) of the prelithiated and unlithiated WO_3 films is determined to be 90.49% and 95.70%, respectively. The difference in two methods for deducting background leads to obvious discrepancy of transmittance modulation between in situ spectra and ex situ spectra. It can be seen that the maximum colored-state transmittance of the prelithiated WO_3 films is about 0.79% (less than the value of 1.17% for the unlithiated WO_3 films), which can be attributed to the larger inserted charge capacity and the presence of 'dead lithium'. In addition, the optical transmittance modulation of the prelithiated WO_3 films shows a 31.63% decline, higher than that of the unlithiated WO_3 films (26.56%). The possible explanation for the dramatical decrease in the optical modulation of the prelithiated WO_3 films is that 'dead lithium' as 'crystal seed' can lead to the accelerated accumulation of 'irreversible lithium', which causes an irreversible damage to optical cycling stability. The coloring/bleaching response time can be described as the time acquired to attain 90% of the maximum transmittance variation [19]. As shown in Fig. 1 (e), the colored time and bleached time is calculated to be 24 s/25 s and 30 s/34 s for the WO_3 films with and without lithiation, respectively. Fig. 1 (f) presents the curves of optical density change (ΔOD) as a function of charge per unit area of the prelithiated and unlithiated WO_3 films. Coloration efficiency (η) as an important electrochromic performance, described as the ratio of optical density variation (ΔOD) and inserted charge density (Q), can be calculated according to the following equation [20]:

$$\eta = \frac{\Delta OD}{Q} = \frac{log(T_b/T_c)}{Q} \tag{3}$$

where T_b and T_c is the optical transmittance of the films in colored state and in bleached state, respectively. The coloration efficiency of the prelithiated WO_3 films is determined to be 36.34 $cm^2\ C^{-1}$, smaller than that (44.81 $cm^2\ C^{-1}$) of the unlithiated WO_3 films. These results demonstrate that the preintercalation of lithium can cause the unobvious transmittance variation under the injection/extraction of the same amount of charge.

To investigate the influence of inserted lithium on the electrochemical performances of the WO_3 films, electrochemical measurements including cyclic voltammetry (CV) and chronocoulometry were performed in the three-electrode system. Fig. 2 (a) and (b) shows CV curves of the prelithiated and unlithiated WO_3 films at various scan rates, respectively. As the scan rate increases, the peak value of current density raises accordingly. Moreover, the peak current density of the prelithiated WO_3 films is larger than that of the unlithiated WO_3 films at the same scan rate, indicating that the conductivity of the films can be enhanced by the preactivation of the intercalated 'active lithium'. Fig. 2 (c) illustrates the curves of the peak current (I_p) as a function of the arithmetic root of the scan rate ($v^{1/2}$) of the prelithiated and unlithiated WO_3 films. The ion diffusion coefficient (D) can be derived from the following Randles-Sevcik law [21]:

$$I_p/A = 2.72 \times 10^5 \times n^{3/2} \times D^{1/2} \times C_0 \times v^{1/2} \tag{4}$$

where n, A and C_0 is the number of electrons ($n = 1$ in Li^+), the area of the working electrode and concentration of active ions in the electrolyte, respectively. The calculated D of the prelithiated and unlithiated WO_3 films is 4.1×10^{-8} and 1.26×10^{-8}, respectively. The intercalated/extracted charge density of the prelithiated and unlithiated WO_3 films can be measured by chronocoulometry measurement, which is carried out at constant penitential of +1.0 V and − 1.0 V with the same duration of 45 s. As illustrated in Fig. 2(d), the intercalated/extracted charge density of the WO_3 films is increased from 37.0/32.4 mC cm^{-2} to 46.3/41.4 mC m^{-2} after lithium-ion intercalation, respectively. The percentage ratio of Q_{in} (intercalated charge) and Q_{ex} (extracted charge) is usually used to evaluate the reversibility of films. It can be seen that the ratio is expanded from 87.6% to 89.4%, demonstrating an enhanced reversibility of the WO_3 films after lithiating. Fig. 2(e) and (f) shows the initial 100 CV curves of the prelithiated and unlithiated WO_3 films in the potential range of −1.0 V to +1.0 V at a scan rate of 100 mV/s, respectively. The nearly coincident CV curves of the prelithiated WO_3 films imply an enhanced electrochemical cycling stability, originating from a synergistic effect of the activation of 'active lithium' and the suppression of 'dead lithium'.

The effect of prelithiation on the charge transfer and ion migration at the WO_3 films/Li^+-based electrolyte interface was examined by using

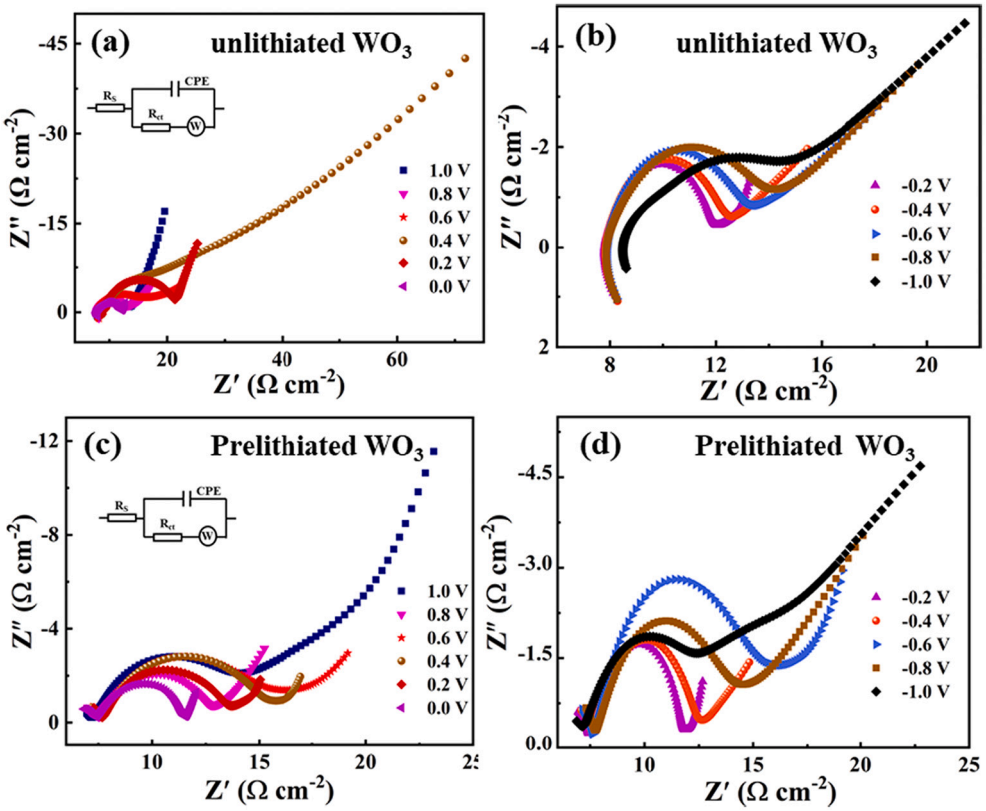

Fig. 3. Nyquist plots for the unlithiated WO_3 films measured at a series of (a) positive voltage and (b) negative voltage. Nyquist plots for the prelithiated WO_3 films measured at a series of positive(c) voltage and (d) negative voltage.

Table 1
A summary of Nyquist measurement for the WO_3 thin films with and without prelithiation in 0.1 M PC-$LiClO_4$ electrolyte.

Applied Potentials	Electrical Parameters			
	R_s (Ω/cm^2)		R_{ct} (Ω/cm^2)	
(V)	unlithiated WO_3 films	prelithiated WO_3 films	unlithiated WO_3 films	prelithiated WO_3 films
+1.0	7.34	7.17	5.28	7.00
+0.8	7.87	7.38	5.13	5.31
+0.6	7.83	7.46	9.29	8.64
+0.4	9.35	7.55	24.95	7.93
+0.2	9.55	7.56	10.92	6.05
0.0	7.82	6.70	3.91	9.61
−0.2	7.88	7.28	4.11	4.61
−0.4	7.93	7.40	4.63	5.35
−0.6	7.97	7.46	5.57	6.26
−0.8	7.98	7.47	6.37	7.63
−1.0	9.06	6.70	8.70	9.66

the electrochemical impedance spectroscopy (EIS) measurements. Fig. 3 (a-d) shows a series of electrochemical impedance spectra of the unlithiated (Fig. 3 (a) and (b)) and prelithiated (Fig. 3(c) and (d)) WO_3 films measured in the frequency range from 100 mHZ to100 KHZ, respectively. As described in Fig. 3 (a) and (c), the slope of these curves in the lower frequency region of both the unlithiated and prelithiated WO_3 films decrease as the applied positive potential increase, indicating that the intercalation of ions is hindered [22,23]. A simplified Randle's equivalent circuit model depicted in the inset of Fig. 3 (a) can be used to evaluate the EIS spectra [24]. The resistance of the Li^+-based electrolyte (R_s), the interfacial charge-transfer resistance (R_{ct}) and W is defined as the intercept between the plot and the real axis in the high frequency region, the diameter of the semicircle and the semi-infinite Warburg element, respectively [25,26]. These fitted resistance values (R_s and R_{ct}) under various applied potential are given in Table 1. The resistance of electrolyte in the prelithiated WO_3 films is slightly lower than that in the unlithiated WO_3 films, indicating that the ionic conductivity of the Li^+-based electrolyte is enhanced. This improvement may be associated with the increment of concentration of Li^+ near the electrolyte/the WO_3 films caused by the extraction of 'active lithium'. Besides, the prelithiated WO_3 films present a series of larger interfacial charge-transfer resistance at the same potential. The possible reason for larger R_{ct} can be attributed to the enlarged surface area, induced by the preintercalation of lithium, which can hinder the process of ion migration due to the increment of active sites.

The ex situ wavelength-dependent spectra of the WO_3-based ECD with and without prelithiation are depicted in Fig. 4 (a). For the WO_3-based ECD with prelithiation, the transmittance spectra of both colored state and bleached state seems to be obviously lower than that of the WO_3-based ECD without prelithiation. The deeper colored state of the WO_3-based ECD with prelithiation can be ascribed to the activation of 'active lithium', which enhances the intercalation of lithium-ion. Moreover, the 'dead lithium' aggravates the accumulation of irreversible lithium, which leads to a decrease in the transmittance of the WO_3-based ECD with prelithiation in bleached state. The maximal transmittance modulation of ECD with and without prelithiation at λ_{633nm} is estimated to be 44.25% and 36.36%, respectively. Fig. 4 (b) shows the in situ time-dependent transmittance spectra of the WO_3-based ECD with and without prelithiation. The transmittance modulation of the ECD with prelithiation is dramatically decrease from 39.35% (1st cycle) to 29.24% (50th), indicating the sacrifice of cycling stability, which can be attributed to the rapid accumulation of irreversible lithium induced by the 'dead lithium seed'. Fig. 4(c) and (d) displays a series of CV curves of the ECD with and without prelithiation at a scan rate of 100 mV/s, respectively. The CV curves of the prelithiated WO_3 films remain almost unchanged in shape, indicating an excellent electrochemical cycling stability. The enhancement of electrochemical stability further confirms

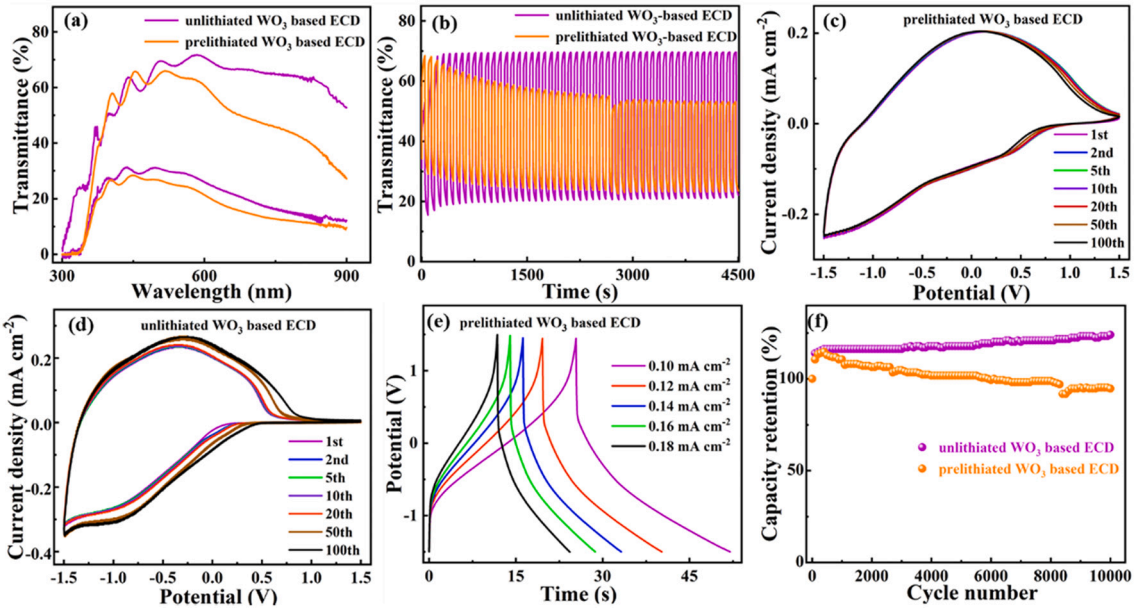

Fig. 4. The ex situ (a) wavelength-dependent and (b) in situ time-dependent transmittance spectra at λ_{633nm} for the WO_3-based complementary ECD with and without prelithiation. First 100 CV curves of the WO_3-based complementary ECD (c) with and (d) without prelithiation. (e) The GCD curves for the WO_3-based ECD with prelithiation at various current densities of 0.10 mA cm^{-2}, 0.12 mA cm^{-2}, 0.14 mA cm^{-2}, 0.16 mA cm^{-2} and 0.18 mA cm^{-2}. (f) Cycling property of the WO_3-based complementary ECD with and without prelithiation at a current density of 0.14 mA cm^{-2}.

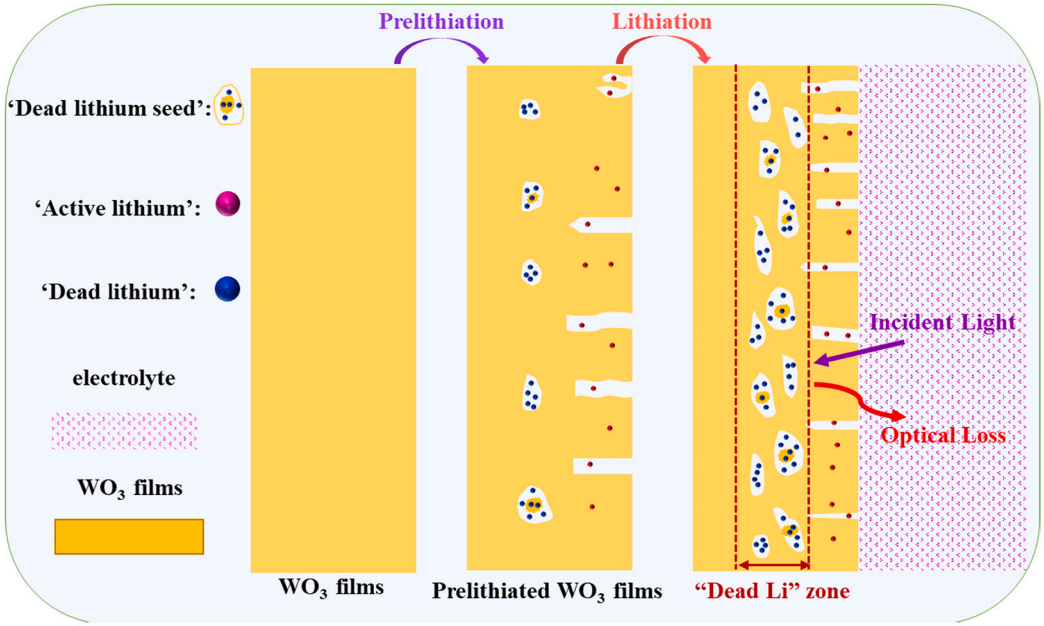

Fig. 5. A schematic illustration of the electrochromic behavior induced by the predeposited lithium of the WO_3 films.

the combined effect of 'active lithium' and 'dead lithium', similar to that in the aforementioned prelithiated WO_3 films. The GCD curves of ECD with prelithiation measured at different current densities are shown in Fig. 4 (e). These curves show a relatively symmetrical characteristic, involving a reversible redox reaction [27]. Fig. 4 (f) illustrates the capacitance retention curves of ECD with and without prelithiation at 0.14 mA cm^{-2} for various cycle numbers. The result shows that the ECD with and without prelithiation holds a capacitance retention ratio of 94.71% and 123.26% after 10,000 cycles. In initial 500 cycles, the capacitance retention of the prelithiated WO_3-based ECD is dramatically increased to 114.71%, owing to the activation of 'active lithium'. The continuous accumulation of 'irreversible lithium', resulting from the 'dead lithium seed' introduced by the prelithiation process, can lead to a declining trend in the capacitance retention. Moreover, the exceptional capacitance retention ratio of the unlithiated WO_3-based ECD can be related to a continuous activation occurred in the host material [28].

The schematic diagram of the effect of the predeposited lithium on the performances of the WO_3 films can be depicted in Fig. 5. 'Lithium vapor' formed by bombarding lithium metal with high-energy electron beam (10 kV) is deposited on the WO_3 films and lithium atoms are thermally diffused into the framework of the host materials at 200 °C. The appearance of the WO_3 films is changed from transparent to light blue. Partial lithium irreversibly located in deep trap, known as 'dead lithium', plays a significant role of 'crystal seed'. The 'crystal seed' can

promote the accumulation of irreversible lithium, resulting in the formation of a 'dead lithium zone' in the WO_3 films which leads to the degradation in the optical performance. In addition, the intercalation/extraction of 'active lithium' in the WO_3 films can expand the number of transporting channel and enlarge the surface area. These variations in the host materials can make a significant contribution to the improvement of electrochemical performances and the increment of R_{ct}.

5. Conclusions

In summary, a novel dry prelithiation of the WO_3 films was carried out by in situ continuous preparation process of electron beam evaporation technique to investigate the influence of the deposited lithium on the electrochromic and electrochemical performances. The inserted lithium is confirmed to be composed of 47.8% 'active lithium' and 52.2% 'dead lithium'. The dry prelithiation shows a positive effect on the improvement of the electrochemical stability of the WO_3 films in lithium electrolytes, which sacrifices its electrochromic properties. The improved electrochemical properties of the prelithiated WO_3 films can be attributed to the enlarged surface area originated from the activation of 'active lithium' after prelithiation. The 'irreversible lithium', induced by the 'dead lithium seed', tends to dramatically accumulate in the WO_3 films to form a 'dead lithium zone', which causes degradation in the optical performances. Scientific insight into the prelithiated films is helpful to introduce a new promising method for fabricating high-performance complementary electrochromic devices.

Author statement

All authors have seen and approved the final version of the manuscript being submitted. We warrant that the article is our original work, hasn't received prior publication and isn't under consideration for publication elsewhere.

Declaration of Competing Interest

The authors declare that they have no known competing financial interests or personal relationships that could have appeared to influence the work reported in this paper.

Acknowledgements

This project is supported by the National Natural Science Foundation of China (61974148 and 61774098) and Ningbo Science and Technology Innovation 2025 Major Special Project (2020Z002).

References

[1] Ö.D. Coşkun, G. Atak, The effects of lithiation process on the performance of all-solid-state electrochromic devices, Thin Solid Films 662 (2018) 13–20.
[2] Y. Ye, J. Zhang, P. Gu, J. Tang, Study on the WO_3 dry lithiation for all-solid-state electrochromic devices, Sol. Energy Mater. Sol. Cells 46 (1997) 349–355.
[3] K. Boufker, Lithiation study of molybdenum oxide thin films: application to an electrochromic system, J. Appl. Electrochem. 25 (1995) 797–802.
[4] J. Zheng, K. Liang, K. Shi, Y. Qiu, In situ synthesis and electrochemical properties of Fe/Li_2O as a high-capacity cathode prelithiation additive for lithium ion batteries, Int. J. Electrochem. Sci. 14 (2019) 5305–5316.
[5] G. Wang, F. Li, D. Liu, D. Zheng, Y. Luo, D. Qu, T. Ding, D. Qu, Chemical prelithiation of negative electrodes in ambient air for advanced lithium-ion batteries, ACS Appl. Mater. Interfaces 11 (2019) 8699–8703.
[6] D. Ruqian, T. Shiyu, Z. Kaicheng, C. Jingrui, Z. Yi, T. Weichao, W. Xiaoyan, W. Lizhi, W. Li, L. Guangchuan, Recent advances in cathode prelithiation additives and their use in lithium–ion batteries, J. Electroanal. Chem. 893 (2021), 115325.
[7] B. Anothumakkool, S. Wiemers-meyer, D. Guyomard, M. Winter, T. Brousse, J. Gaubicher, Cascade-type prelithiation approach for Li-ion capacitors, Adv. Energy Mater. 9 (2019) 1900078.
[8] S.S. Zhang, Eliminating pre-lithiation step for making high energy density hybrid Li-ion capacitor, J. Power Sources 343 (2017) 322–328.
[9] G. Viera Porqueras, J. Marti, E. Bertran, Deep profiles of lithium in electrolytic structures of ITO/WO_3 for electrochromic applications, Thin Solid Films 343 (1999) 179–182.
[10] R.D. Rauh, Electrochromic windows: an overview, Electrochim. Acta 44 (1999) 3165–3176.
[11] B.A. Samad, P.V. Ashrit, The dependence of electrical conductivity on temperature for dry lithiated crystalline tungsten trioxide thin films, Solid State Ionics 308 (2017) 156–160.
[12] W. Caiping, D. Guobo, Z. Yuyang, H. Yingchun, D. Yilin, D. Xinpan, Z. Xiaolan, W. Mei, D. Xungang, Enhanced electrochromic performance on anodic nickel oxide inorganic device via lithium and aluminum co-doping, J. Alloys Compd. 821 (2020), 153365.
[13] P.V. Ashrit, Dry lithiation study of nanocrystalline, polycrystalline and amorphous tungsten trioxide thin-films, Thin Solid Films 385 (2001) 81–88.
[14] D. Qiu, H. Ji, X. Zhang, H. Zhang, H. Cao, G. Chen, T. Tian, Z. Chen, X. Guo, L. Liang, J. Gao, F. Zhuge, Electrochromism of nanocrystal-in-glass tungsten oxide thin films under various conduction cations, Inorg. Chem. 58 (2019) 2089–2098.
[15] K. Wang, D. Qiu, H. Zhang, G. Chen, W. Xie, K. Tao, S. Bao, L. Liang, J. Gao, H. Cao, Boosting charge-transfer kinetics and cyclic stability of complementary WO_3–NiO electrochromic devices via SnO_x interfacial layer, J. Dermatol. Sci. 6 (2021) 494–500.
[16] G. Beydaghyan, G. Bader, P.V. Ashrit, Electrochromic and morphological investigation of dry-lithiated nanostructured tungsten trioxide thin films, Thin Solid Films 516 (2008) 1646–1650.
[17] W. Li, X. Zhang, X. Chen, Y. Zhao, L. Wang, M. Chen, Z. Li, J. Zhao, Y. Li, Lithiation of WO_3 films by evaporation method for all-solid-state electrochromic devices, Electrochim. Acta 355 (2020), 136817.
[18] O. Bouvard, M. Lagier, L. Burnier, A. Krammer, A. Schüler, Strong coloration of nanoporous tungsten oxides by in-vacuo lithiation for all-solid-state electrochromic devices, Thin Solid Films 730 (2021), 138700.
[19] Y. Shi, M. Sun, Y. Zhang, J. Cui, Y. Wang, X. Shu, Y. Qin, H.H. Tan, J. Liu, Y. Wu, Structure modulated amorphous/crystalline WO_3 nanoporous arrays with superior electrochromic energy storage performance, Sol. Energy Mater. Sol. Cells 212 (2020), 110579.
[20] S. Heo, C.J. Dahlman, C.M. Staller, T. Jiang, A. Dolocan, B.A. Korgel, D.J. Milliron, Enhanced coloration efficiency of electrochromic tungsten oxide nanorods by site selective occupation of sodium ions, Nano Lett. 20 (2020) 2072–2079.
[21] B. Zhao, S. Lu, X. Zhang, H. Wang, J. Liu, H. Yan, Porous WO_3/reduced graphene oxide composite film with enhanced electrochromic properties, Ionics 22 (2015) 261–267.
[22] Y. Wang, R. Zheng, J. Luo, H.A. Malik, Z. Wan, C. Jia, X. Weng, J. Xie, L. Deng, X. Yao, Self-healing dynamically cross linked versatile polymer electrolyte: a novel approach towards high performance, flexible electrochromic devices, Electrochim. Acta 320 (2019), 134489.
[23] K. Wang, H. Zhang, G. Chen, T. Tian, K. Tao, L. Liang, J. Gao, H. Cao, Long-term-stable WO_3-PB complementary electrochromic devices, J. Alloys Compd. 861 (2021), 158534.
[24] P.T.G. Gayathri, S. Sajitha, I. Vijitha, S.S. Shaiju, R. Remya, B. Deb, Tuning of physical and electrochemical properties of nanocrystalline tungsten oxide through ultraviolet photoactivation, Electrochim. Acta 272 (2018) 135–143.
[25] M. Jamdegni, A. Kaur, Electrochromic behavior of highly stable, flexible electrochromic electrode based on covalently bonded polyaniline-graphene quantum dot composite, J. Electrochem. Soc. 166 (2019) H502–H509.
[26] K. Li, Y. Shao, S. Liu, Q. Zhang, H. Wang, Y. Li, R.B. Kaner, Aluminum-ion-intercalation supercapacitors with ultrahigh areal capacitance and highly enhanced cycling stability: power supply for flexible electrochromic devices, Small 13 (2017) 1700380.
[27] S. Zhou, C. Hao, J. Wang, X. Wang, H. Gao, Metal-organic framework templated synthesis of porous $NiCo_2O_4$/$ZnCo_2O_4$/Co_3O_4 hollow polyhedral nanocages and their enhanced pseudocapacitive properties, Chem. Eng. J. 351 (2018) 74–84.
[28] H. Chen, M. Zhou, Z. Wang, S. Zhao, S. Guan, Rich nitrogen-doped ordered mesoporous phenolic resin-based carbon for supercapacitors, Electrochim. Acta 148 (2014) 187–194.